Topological Phononic Logic

Harris Pirie,[1] Shuvom Sadhuka,[2] Jennifer Wang,[2,3] and Jennifer E. Hoffman[1,2]

[1] *Department of Physics, Harvard University, Cambridge, MA, 02138, USA*
[2] *School of Engineering and Applied Science, Harvard University, Cambridge, MA, 02138, USA*
[3] *Department of Physics, Wellesley College, Wellesley MA, 02481, USA*

(Dated: September 26, 2018)

Topological metamaterials have robust properties engineered from their macroscopic arrangement, rather than their microscopic constituency. They are promising candidates for creating next-generation technologies due to their protected dissipationless boundary modes. They can be designed by starting from Dirac metamaterials with either symmetry-enforced or accidental degeneracy. The latter case provides greater flexibility in the design of topological switches, waveguides, and cloaking devices, because a large number of tuning parameters can be used to break the degeneracy and induce a topological phase. However, the design of a topological logic element—a switch that can be controlled by the output of a separate switch—remains elusive. Here we numerically demonstrate a topological logic gate for ultrasound by exploiting the large phase space of accidental degeneracies in a honeycomb lattice. We find that a degeneracy can be broken by six physical parameters, and we show how to tune these parameters to create a phononic switch between a topological waveguide and a trivial insulator that can be triggered by ultrasonic heating. Our design scheme is directly applicable to photonic crystals and may guide the design of future electronic topological transistors.

1 Topological insulators were first conceived as quantum electronic materials with insulating bulk and surface Dirac states allowing for dissipationless charge and spin transport along their boundaries. Their central principle—the inversion of energy bands—is also present in many classical lattice systems, inspiring the design of photonic [1–3], phononic [4], and mechanical metamaterials [5–7] with topologically protected transport. These classical systems provide a platform to test ideas in topological band theory, because they are more tangibly understood than their quantum counterparts, and their governing wave equations can be solved exactly. Their robust properties have been used in many promising applications including zero- and negative-refractive-index materials [8–12], cloaking [13, 14], and dissipationless waveguides for sound and light that outperform non-topological alternatives [15–20]. Here we demonstrate three tiers of topological phononic metamaterials, building from a static-geometry waveguide, to an externally switchable device, and ultimately to logic circuits.

2 A general design approach to achieve the band inversion that defines a topological metamaterial is to start from a bulk Dirac state, then intentionally break the Dirac-point degeneracy to open a negative gap. This approach can be broadly divided into two methods. The first method starts from a symmetry-enforced Dirac state, such as the K-point Dirac cone in graphene-like honeycomb or triangular metamaterials, then opens a gap by breaking a symmetry of the system. In systems with broken time-reversal ($\mathcal{T}$) symmetry [21–25], the resultant topological phase is analogous to the quantum Hall effect, while those with broken translational symmetry [18, 20, 26–29] can realize an analog of the quantum spin Hall effect. However, there is limited flexibility in the design of these topological phases, as they can be tuned only by a symmetry-breaking operation. On the other hand, the second method searches for the accidental degeneracy of three [8, 14, 30] or four [9, 31, 32] bands, producing a Dirac-like cone or double Dirac cones, respectively. This method gives access to a far larger set of topological phases because the accidental degeneracy can be broken by many more accessible tuning parameters while retaining translational and $\mathcal{T}$ symmetry. Despite the utility and flexibility of this method, the complete space of all topological phases has yet to be mapped for any accidental degeneracy.

3 We start from a particular accidental bulk Dirac-point degeneracy that gives rise to a topological state analogous to a quantum spin Hall system. In a quantum spin Hall system, the protection of the Dirac point is a consequence of the spin-$1/2$ nature of electrons. Specifically, because $\mathcal{T}^2 = -1$ for spin-$1/2$ states, Kramers theorem requires a degeneracy at all $\mathcal{T}$-invariant points of the Brillouin zone. However, spin-0 phononic and spin-1 photonic systems both have $\mathcal{T}^2 = +1$ so Kramers theorem does not apply. Instead, designs typically rely on mode hybridization to form a pseudospin-$1/2$ subsystem, for example with the transverse electric and magnetic polarizations of light [2]. But transverse shear modes are not available in airborne acoustics, so finding an analogy of Kramers theorem is challenging. In 2012, Sakoda [31] addressed this issue and constructed a pseudospin-$1/2$ system using the discrete symmetries of a triangular lattice, which was adapted to longitudinal acoustic modes shortly thereafter [9, 32, 33] and subsequently demonstrated experimentally [16]. In this scheme, a lattice with C_{6v} symmetry generates an accidental degeneracy at the Γ point between doubly degenerate E_1 and E_2 modes that transform as (x, y) and $(xy, x^2 - y^2)$. These modes are denoted (p_x, p_y) and $(d_{xy}, d_{x^2-y^2})$, due to their sim-

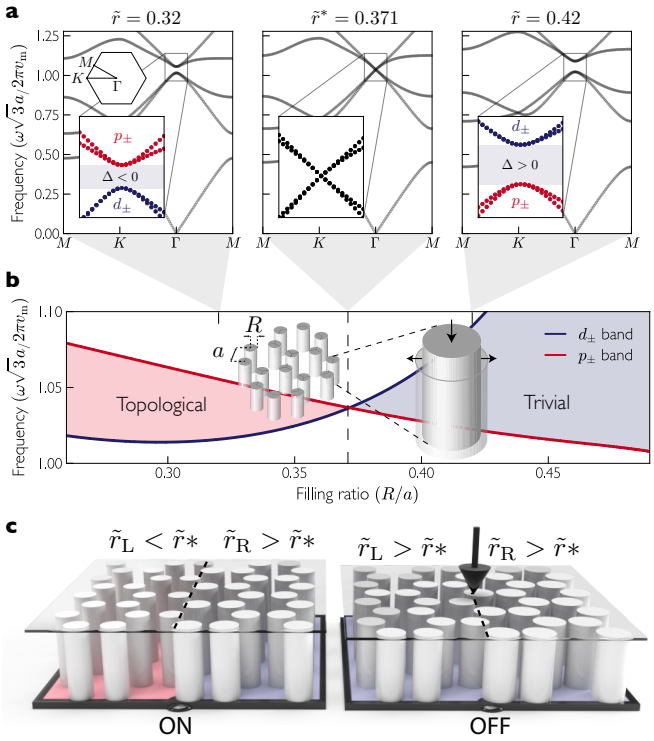

FIG. 1. **An externally controlled topological switch for sound.** (**a**) The phononic band structure for a honeycomb lattice of steel pillars in water passes through an accidental degeneracy as the radius of the pillars is varied. This degeneracy is between $p_\pm$ bands (red) and $d_\pm$ bands (blue), and occurs at the critical filling ratio of $\tilde{r}^* \equiv R/a = 0.371$ (middle panel). As the filling ratio is tuned away from this value a positive (right) or negative (left) band gap is opened, leading to a topological phase transition. (**b**) The topological phase transition can be clearly seen by tracking the Γ-point eigenvalues as $\tilde{r}$ is tuned. (**c**) A topological waveguide is made from placing two lattices with $\tilde{r_L} < \tilde{r}^*$ and $\tilde{r_R} > \tilde{r}^*$ next to each other (left panel). When the pillars are compressed vertically, their radius expands due to the positive Poisson's ratio of steel, such that both sides of the waveguide become trivial insulators (right panel). This device constitutes a topological switch for sound that turns 'off' when compressed.

ilarity with electronic states. These doubly degenerate modes allow the formation of a pseudo-spin-1/2 basis, with corresponding eigenstates $p_\pm = (p_x \pm ip_y)/\sqrt{2}$ and $d_\pm = (d_{x^2-y^2} \pm id_{xy})/\sqrt{2}$. The accidental degeneracy between the $p_\pm$ and $d_\pm$ subsystems can be lifted without breaking C_{6v} symmetry, allowing the system to realize a topological phase with helical edge modes protected by a pseudo-$\mathcal{T}$ symmetry, analogous to the quantum spin Hall state.

4 Here we numerically investigate the topological phase space for a Γ-point accidental degeneracy in a phononic honeycomb lattice using commercial finite-element modelling software COMSOL MULTIPHYSICS. We find a manifold of system configurations that host a bulk accidental double-Dirac cone, and we demonstrate that a topological phase can be induced by gapping the Dirac node with six independent physical parameters, which collapse into a three-dimensional (3D) phase space. By tuning within this phase diagram, we design a topological phononic switch—a dissipationless waveguide for ultrasound that is turned 'on' when heated. Finally, we show schematically how to link several switches together to form a topological NAND gate—the building block of a topological logic circuit.

Results

Externally controlled topological switches

5 In phononic crystals, topologically protected boundary modes exist at the interface between a lattice with normally ordered bands and one with inverted bands. Such boundary modes were previously realized between two hexagonal lattices of steel pillars in a fluid medium with different filling ratios, $\tilde{r} = R/a$ [16, 32], where R and a are the radius and spacing of the pillars, respectively (see inset to Fig. 1(b)). When the filling ratio is large, the band structure around the Γ point contains doubly degenerate $p_\pm$ modes separated from $d_\pm$ modes by a positive energy gap, $\Delta > 0$, as shown in Fig. 1(a). At the critical filling ratio of $\tilde{r}^* = 0.371$ the four modes become accidentally degenerate and the bulk metamaterial hosts double Dirac cones. Below critical filling, the $p_\pm$ have higher energy than the $d_\pm$ modes: the band structure contains a negative energy gap, $\Delta < 0$, giving rise to topologically protected edge modes. These edge modes are confined to the interface between a positive- and negative-gapped material, allowing the design of topological waveguides that are pseudospin polarized and immune to defects including cavities, bends and lattice disorder [16].

6 Our first advance is the demonstration of an externally switchable topological waveguide for sound, which hosts dissipationless transport when 'on', but is a trivial insulator when 'off'. In general, a topological switch requires a tuning mechanism capable of changing the sign of the band gap on the topological side, while leaving that on the trivial side unchanged. For example, an external vertical compression will normally increase the radius of a pillar, as most materials have a positive Poisson's ratio (see inset to Fig. 1(b)). This expansion can alter the topological phase of a honeycomb metamaterial and may be used to construct a topological switch. Specifically, a topological waveguide is switched 'off' when the filling ratio of its topological side increases beyond $\tilde{r}^*$, as shown in Fig. 1(c). Advancing beyond static-geometry topological waveguides [15–20], this type of switch could be used to control passive acoustic isolation systems, but the output of one switch cannot sustain the macroscopic stretch required to activate a second, similar switch.

Phononically controlled topological switches

7 Our second, more significant advance is to design a phononically controlled acoustic switch—i.e. a topologi-

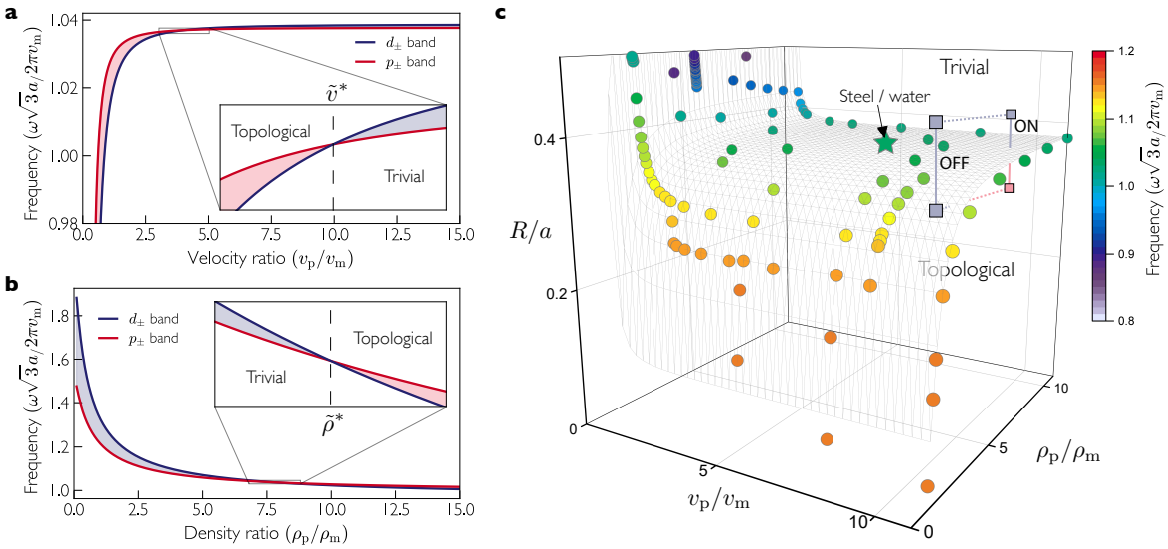

FIG. 2. **Topological phase space in a honeycomb phononic lattice.** An accidental degeneracy between the $p_\pm$ and $d_\pm$ modes in the steel/water lattice demarcated by a green star can be broken by tuning the ratio of (**a**) speed of sound while holding radius and density fixed; or (**b**) density while holding speed of sound and radius fixed. (**c**) Each accidental degeneracy is a point in $(\tilde{r}, \tilde{\rho}, \tilde{v})$ space, colored according to its crossing frequency. Together, this set of points separates phase space into a topological and a trivial region. A topological waveguide exists at the interface between two metamaterials from different sides of this surface (see solid line path labelled ON), provided their bulk spectral gaps overlap. Transmission through such a waveguide can be switched 'off' by tuning the system along the dashed lines to two sets of parameters that occur on the same side of the surface (see solid line path labelled OFF).

cal logic element. Like electronic field-effect transistors, these switches may be connected together to form circuits. Here we rely explicitly on the flexibility granted by the large phase space of accidental degeneracies in a honeycomb metamaterial. In general, an accidental band degeneracy can be lifted by tuning any lattice parameter, as it is not protected by symmetry. The relevant parameters in a phononic lattice define the acoustic wave equation,

$$\boldsymbol{\nabla} \cdot \left[\frac{1}{\rho_r(\mathbf{r})} \boldsymbol{\nabla} p(\mathbf{r}) \right] = -\frac{\omega^2}{v_m^2} \cdot \frac{p(\mathbf{r})}{v_r^2(\mathbf{r}) \rho_r(\mathbf{r})} \qquad (1)$$

where p is the pressure, ω is the eigenfrequency, and $\rho_r(\mathbf{r}) = \rho(\mathbf{r})/\rho_m$ and $v_r(\mathbf{r}) = v(\mathbf{r})/v_m$ are the relative density and speed of sound, respectively. In total, there are six physical parameters that can tune the resulting eigenspectrum: R, a, ρ_p, ρ_m, v_p, and v_m, where the subscript refers to pillars or medium. First note that uniformly scaling ρ_p and ρ_m produces no change, while uniformly scaling v_p and v_m scales all eigenfrequencies of Eq. 1, but does not shift eigenfrequencies relative to one another, and therefore cannot induce a topological phase change. This scaling is taken into account by adopting dimensionless units for frequency, $\tilde{\omega} = \omega a_0/2\pi v_m$. In fact, the frequency-normalized band structure depends only on three dimensionless ratios: $\tilde{r} = R/a$, $\tilde{v} = v_p/v_m$ and $\tilde{\rho} = \rho_p/\rho_m$. In the example system of steel pillars in water, we find that varying either $\tilde{v}$ or $\tilde{\rho}$ lifts the accidental degeneracy and can open a negative gap (Fig. 2(a-b)). More generally, varying any combination of lattice parameters along a path in $(\tilde{v}, \tilde{\rho}, \tilde{r})$ space that connects the topological phase to the trivial phase must pass through an accidental degeneracy. Consequently, there exists a surface in $(\tilde{v}, \tilde{\rho}, \tilde{r})$ space that separates the topological phase from the trivial phase, on which there is accidental degeneracy between $p_\pm$ and $d_\pm$ modes and a bulk double Dirac cone. We numerically calculated the shape of this surface, shown in Fig. 2(c), by recording the accidental crossing point in an $\tilde{r}$ sweep for a discrete set of $(\tilde{v}, \tilde{\rho})$ points, at fixed (v_m, ρ_m).

8 A key challenge in designing a topological switch is to preserve overlapping bulk spectral gaps before and after switching. For example, in the sweep shown in Fig. 2(a), increasing $\tilde{v}$ causes both $p_\pm$ and $d_\pm$ modes to increase in frequency, leading to a band inversion because the $d_\pm$ modes increase faster than the $p_\pm$ modes. Yet, this tuning parameter alone cannot be used to design a topological waveguide because at any frequency there are bulk modes in one of the two sides that mask the edge states, unlike Fig. 1(b). The same accidental degeneracy can be broken by varying $\tilde{\rho}$, which causes both $p_\pm$ and $d_\pm$ modes to decrease in frequency (Fig. 2(b)), again precluding a usefully overlapping gap. However, an overlapping bulk gap can be constructed by tuning $\tilde{v}$ and $\tilde{\rho}$ simultaneously. For example, a successful waveguide could be constructed at the interface between two sets of pillars with different materials, but the same radius. In general, each accidental degeneracy on the surface in Fig. 2(c)

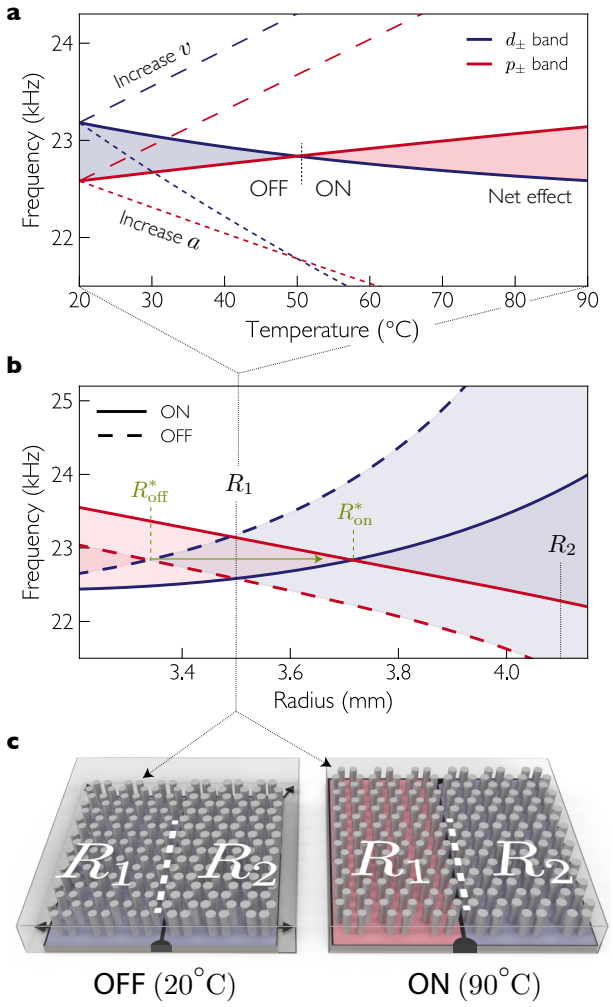

FIG. 3. **Designing a temperature-controlled topological switch.** We consider a honeycomb lattice of steel pillars anchored to a high-thermal-expansion base plate, in an air medium within a sealed box of fixed size. (**a**) Heating this system has two main competing effects: eigenfrequencies are increased by raising the speed of sound in air (dashed lines), but decreased as the base plate thermally expands (dotted lines). The latter effect also tunes $\tilde{r}$ and induces a band inversion. These two effects can be balanced by correctly choosing the thermal expansion coefficient of the base plate (here 1.61×10^{-3} K^{-1}), providing a temperature-tunable topological phase transition with an overlapping spectral gap (solid lines). (**b**) A topological switch combines two lattices of pillars: one side that transitions from trivial to topological as the switch is heated (R_1), and another side that remains trivial throughout the process (R_2). (**c**) Unlike the switch design in Fig. 1 (c), which is triggered by tuning R at fixed a, this switch is turned 'on' by increasing a at fixed R, and can be actuated by phonon-delivered heat.

can be used to construct a practical topological waveguide for a parameter sweep through some solid angle in $(\tilde{v}, \tilde{\rho}, \tilde{r})$ space. Such a waveguide combines two points in parameter space connected by a path that punctures the surface in Fig. 2(c). Correspondingly, a topological switch combines four points in phase space, with three above the surface (trivial) and one below (topological), e.g. the square points in Fig. 2(c). Furthermore, a useful switch requires the bulk to remain gapped and overlapping on all four $(\tilde{v}, \tilde{\rho}, \tilde{r})$ trajectories that connect these points, except when they pass through the surface.

9 To enable the output of one switch to control the next, our design for a phononically-controlled topological switch uses a temperature increase delivered by ultrasonic phonons as the tuning mechanism. Our device consists of a honeycomb lattice of steel pillars attached to a base plate made from a second material, in an air-tight container, as shown in Fig. 3(c). The primary effect of heating the device is to change the speed of sound in the medium, which typically increases all eigenfrequencies of the system (see dashed lines in Fig. 3(a)). Secondly, heating usually causes thermal expansion of the materials, which increases both R and a, but not necessarily by the same amount. If the base plate and pillar materials are selected such that a increases faster than R, the net result is to reduce all eigenfrequencies of the system and induce a band inversion (dotted lines in Fig. 3(a)). Finally, heating alters the density of the air and the materials, which has been taken into account, but is insignificant. The first two effects can be balanced to maintain a bulk gap throughout the switching process, by keeping the ratio $v_{\rm m}/a$ that appears in the eigenfrequency of Eq. 1 fixed. Because the base plate expands linearly with temperature, we seek a medium where $v_{\rm m}$ also increases linearly. For an ideal gas at temperature T, $v_{\rm m}$ increases as $\sqrt{T}$, but becomes close to linear near room temperature; as such, air is a suitable medium. Consequently, to keep $v_{\rm m}/a$ fixed as the temperature increases from T_i to T_f, we seek a base material with a coefficient of thermal expansion given by $\alpha = 1/(T_i + \sqrt{T_i T_f})$.

10 A specific design for a topological phononic switch contains two lattices of steel pillars with radii $R_1 = 3.5$ mm, $R_2 = 4.1$ mm, and spacing $a = 8.5$ mm. The switch operates between 20°C (off) and 90°C (on), and requires the base plate to have a thermal expansion coefficient of 1.61×10^{-3} K^{-1}, which is within the range achievable by origami metamaterials [34]. Alternatively, a shape-memory alloy, such as nitinol, could be used to thermally actuate the base plate over this temperature range. At 20°C, the switch is 'off' because both radii correspond to trivial insulators (dashed lines in Fig. 3(b)). Heating it causes the accidental degeneracy at $R^*_{\rm off}$ to move above R_1 inducing a negative gapped phase on that side (solid lines in Fig. 3(b)). The advantage of a topological phononic switch can be seen from the finite-sized calculations in Fig. 4. Unlike a trivial waveguide, which experiences losses induced by disorder and bends (Fig. 4(a-b)), the topological switch acts as a robust pseudospin-dependent waveguide when 'on' due to a Dirac cone between the two sides (Fig. 4(c-d)). As it is cooled, the pillars contract around the input terminal; both sides

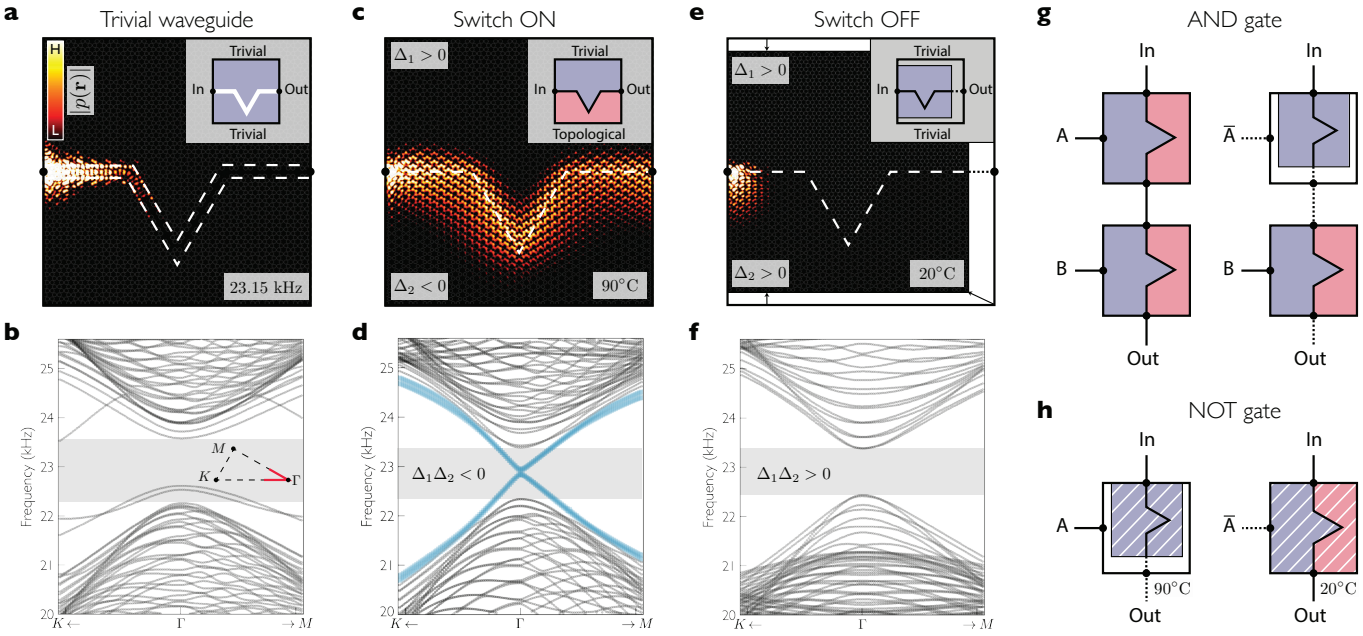

FIG. 4. **Topological logic gates with ultrasound.** (**a**) Transmission through a trivial waveguide, like this channel in an insulating phononic crystal, is disrupted by disorder and bends. (**b**) The corresponding band structure close to the Γ point shows a bulk gap with trivial edge states. (**c**) In contrast, a topological waveguide allows robust transport regardless of channel geometry: it can be used as the 'on' state for a topological switch. This waveguide occurs at the interface between two lattices of steel rods with different radii in an air medium. (**d**) The band structure hosts Dirac-like states (blue) localized at the interface due to a negative bulk gap on one side. (**e-f**) When the system is cooled, it contracts and both sides become trivial insulators. In this configuration the topological switch is 'off' and excitations decay exponentially into the bulk. (**g**) A topological AND gate can be constructed by connecting two switches in series. A signal can propagate from input to output only when both the control signals (A and B) are present. (**h**) This schematic for a NOT gate uses a base plate with a negative thermal expansion coefficient to contract and turn 'off' when heated (left), and expand to turn 'on' when cooled (right). Together, the devices in (g) and (h) can be combined to construct an arbitrary logic gate for ultrasound.

become insulating and block transmission, turning the switch 'off' (Fig. 4(e-f)).

Discussion

11 To establish logic capability, it is necessary to demonstrate only a NAND gate, from which any arbitrary logic gate can be formed. First, we realize a topological AND gate by connecting two phononically controlled switches in series, as shown in Fig. 4(g). This device requires both control signals (A and B) to be 'on', in order to heat each of the two switches and allow information to propagate. Second, to design a topological NOT gate, we utilize a base plate material that has a negative coefficient of thermal expansion; it shrinks when heated. At room temperature (control is 'off') the NOT gate is a topological waveguide that transmits information. With the control 'on', the device heats and shrinks, transitioning to a trivial insulator. To maintain an overlapping bulk gap throughout this transition we require a medium in which the speed of sound decreases with increasing temperature, a behaviour commonly observed oils [35]. Specifically, a device using steel pillars in sunflower oil requires a coefficient of thermal expansion of -2.0×10^{-3} K^{-1} to keep the ratio v_m/a fixed and to maintain an overlapping bulk gap. Such a thermal expansion coefficient was recently demonstrated using origami metamaterials [34].

12 The design of topological metamaterials based on accidental degeneracy is extremely versatile due to the large number of tuning parameters available. For an accidental degeneracy in a phononic honeycomb lattice, we showed that the topological phase can be tuned by six independent parameters, which collapse onto a 3D phase space. This space guided the design of a phononically controlled topological switch that could form the basis of an acoustic logic gate. Additionally, the topological phases we have predict will allow the design of zero-refractive-index metamaterials and acoustic cloaks, due to the placement of the accidental degeneracy around the Γ point [13, 14]. Finally, our conclusions directly apply to optical systems under a simple mapping of variables [30] and motivate further exploration of the topological phases around accidental degeneracies in quantum materials, which may lead to the development of a field-effect topological transistor.

Acknowledgements We thank Katia Bertoldi, Barbara Dorritie, Jason Hoffman, David Lee, Ciarán O'Neill, Pai Wang, and Jack Zhang for helpful conversations. This work was supported by the Science and Technology Center for Integrated Quantum Materials under the National Science Foundation grant No. DMR-1231319.

Author Contributions S.S. and J.W. performed COMSOL calculations. H.P. and J.H. conceived and supervised the project. H.P. wrote the manuscript with substantive input from all authors.

Author Information The authors declare that they have no competing financial interests.

Correspondence and requests for materials should be addressed to H.P. (hpirie@g.harvard.edu) and J.E.H. (jhoffman@physics.harvard.edu).

[1] F. D. M. Haldane and S. Raghu, "Possible Realization of Directional Optical Waveguides in Photonic Crystals with Broken Time-Reversal Symmetry," Physical Review Letters **100**, 013905 (2008).

[2] Alexander B. Khanikaev, S. Hossein Mousavi, Wang-Kong Tse, Mehdi Kargarian, Allan H. MacDonald, and Gennady Shvets, "Photonic topological insulators," Nature Materials **12**, 233–239 (2013).

[3] Ling Lu, John D. Joannopoulos, and Marin Soljačić, "Topological photonics," Nature Photonics **8**, 821–829 (2014).

[4] Hao Ge, Min Yang, Chu Ma, Ming-Hui Lu, Yan-Feng Chen, Nicholas Fang, and Ping Sheng, "Breaking the barriers: Advances in acoustic functional materials," National Science Review **5**, 159–182 (2018).

[5] C. L. Kane and T. C. Lubensky, "Topological boundary modes in isostatic lattices," Nature Physics **10**, 39–45 (2014).

[6] R. Susstrunk and S. D. Huber, "Observation of phononic helical edge states in a mechanical topological insulator," Science **349**, 47–50 (2015).

[7] Sebastian D. Huber, "Topological mechanics," Nature Physics **12**, 621–623 (2016).

[8] Fengming Liu, Xueqin Huang, and C. T. Chan, "Dirac cones at k→=0 in acoustic crystals and zero refractive index acoustic materials," Applied Physics Letters **100**, 071911 (2012).

[9] Yan Li, Ying Wu, and Jun Mei, "Double Dirac cones in phononic crystals," Applied Physics Letters **105**, 014107 (2014).

[10] Marc Dubois, Chengzhi Shi, Xuefeng Zhu, Yuan Wang, and Xiang Zhang, "Observation of acoustic Dirac-like cone and double zero refractive index," Nature Communications **8**, 14871 (2017).

[11] Iñigo Liberal and Nader Engheta, "Near-zero refractive index photonics," Nature Photonics **11**, 149–158 (2017).

[12] Hailong He, Chunyin Qiu, Liping Ye, Xiangxi Cai, Xiying Fan, Manzhu Ke, Fan Zhang, and Zhengyou Liu, "Topological negative refraction of surface acoustic waves in a Weyl phononic crystal," Nature **560**, 61–64 (2018).

[13] Jiaming Hao, Wei Yan, and Min Qiu, "Super-reflection and cloaking based on zero index metamaterial," Applied Physics Letters **96**, 101109 (2010).

[14] Xueqin Huang, Yun Lai, Zhi Hong Hang, Huihuo Zheng, and C. T. Chan, "Dirac cones induced by accidental degeneracy in photonic crystals and zero-refractive-index materials," Nature Materials **10**, 582–586 (2011).

[15] S. Hossein Mousavi, Alexander B. Khanikaev, and Zheng Wang, "Topologically protected elastic waves in phononic metamaterials," Nature Communications **6**, 8682 (2015).

[16] Cheng He, Xu Ni, Hao Ge, Xiao-Chen Sun, Yan-Bin Chen, Ming-Hui Lu, Xiao-Ping Liu, and Yan-Feng Chen, "Acoustic topological insulator and robust one-way sound transport," Nature Physics **12**, 1124–1129 (2016).

[17] Qi Wei, Ye Tian, Shu-Yu Zuo, Ying Cheng, and Xiao-Jun Liu, "Experimental demonstration of topologically protected efficient sound propagation in an acoustic waveguide network," Physical Review B **95**, 094305 (2017).

[18] Bai-Zhan Xia, Ting-Ting Liu, Guo-Liang Huang, Hong-Qing Dai, Jun-Rui Jiao, Xian-Guo Zang, De-Jie Yu, Sheng-Jie Zheng, and Jian Liu, "Topological phononic insulator with robust pseudospin-dependent transport," Physical Review B **96**, 094106 (2017).

[19] Zhiwang Zhang, Ye Tian, Ying Cheng, Xiaojun Liu, and Johan Christensen, "Experimental verification of acoustic pseudospin multipoles in a symmetry-broken snowflakelike topological insulator," Physical Review B **96**, 241306 (2017).

[20] Yuting Yang, Yun Fei Xu, Tao Xu, Hai-Xiao Wang, Jian-Hua Jiang, Xiao Hu, and Zhi Hong Hang, "Visualization of a Unidirectional Electromagnetic Waveguide Using Topological Photonic Crystals Made of Dielectric Materials," Physical Review Letters **120**, 217401 (2018).

[21] Zheng Wang, Yidong Chong, J. D. Joannopoulos, and Marin Soljačić, "Observation of unidirectional backscattering-immune topological electromagnetic states," Nature **461**, 772–775 (2009).

[22] R. Fleury, D. L. Sounas, C. F. Sieck, M. R. Haberman, and A. Alu, "Sound Isolation and Giant Linear Nonreciprocity in a Compact Acoustic Circulator," Science **343**, 516–519 (2014).

[23] Zhaoju Yang, Fei Gao, Xihang Shi, Xiao Lin, Zhen Gao, Yidong Chong, and Baile Zhang, "Topological Acoustics," Physical Review Letters **114**, 114301 (2015).

[24] Pai Wang, Ling Lu, and Katia Bertoldi, "Topological Phononic Crystals with One-Way Elastic Edge Waves," Physical Review Letters **115**, 104302 (2015).

[25] Lisa M. Nash, Dustin Kleckner, Alismari Read, Vincenzo Vitelli, Ari M. Turner, and William T. M. Irvine, "Topological mechanics of gyroscopic metamaterials," Proceedings of the National Academy of Sciences **112**, 14495–14500 (2015).

[26] Long-Hua Wu and Xiao Hu, "Scheme for Achieving a Topological Photonic Crystal by Using Dielectric Material," Physical Review Letters **114**, 223901 (2015).

[27] Zhiwang Zhang, Qi Wei, Ying Cheng, Ting Zhang, Dajian Wu, and Xiaojun Liu, "Topological Creation of Acoustic Pseudospin Multipoles in a Flow-Free Symmetry-Broken Metamaterial Lattice," Physical Review Letters **118**, 084303 (2017).

[28] Yuanchen Deng, Hao Ge, Yuan Tian, Minghui Lu, and Yun Jing, "Observation of zone folding induced acoustic topological insulators and the role of spin-mixing defects," Physical Review B **96**, 184305 (2017).

[29] Zhiwang Zhang, Ye Tian, Ying Cheng, Qi Wei, Xiaojun Liu, and Johan Christensen, "Topological Acoustic Delay Line," Physical Review Applied **9**, 034032 (2018).
[30] Jun Mei, Ying Wu, C. T. Chan, and Zhao-Qing Zhang, "First-principles study of Dirac and Dirac-like cones in phononic and photonic crystals," Physical Review B **86**, 035141 (2012).
[31] Kazuaki Sakoda, "Double Dirac cones in triangular-lattice metamaterials," Optics Express **20**, 9925 (2012).
[32] Ze-Guo Chen, Xu Ni, Ying Wu, Cheng He, Xiao-Chen Sun, Li-Yang Zheng, Ming-Hui Lu, and Yan-Feng Chen, "Accidental degeneracy of double Dirac cones in a phononic crystal," Scientific Reports **4**, 4613 (2015).
[33] Jun Mei, Zeguo Chen, and Ying Wu, "Pseudo-time-reversal symmetry and topological edge states in two-dimensional acoustic crystals," Scientific Reports **6**, 32752 (2016).
[34] Elisa Boatti, Nikolaos Vasios, and Katia Bertoldi, "Origami Metamaterials for Tunable Thermal Expansion," Advanced Materials **29**, 1700360 (2017).
[35] P A Oliveira, R M B Silva, G C Morais, A V Alvarenga, and R P B Costa Félix, "Speed of sound as a function of temperature for ultrasonic propagation in soybean oil," Journal of Physics: Conference Series **733**, 012040 (2016).